JOURNAL OF SOLID STATE CHEMISTRY 119, 13–23 (1995)

Interconversion of CrO_2 Formed by Decomposition of Chromium(III) Nitrate Nonahydrate

M. Maciejewski, K. Köhler,[1] H. Schneider, and A. Baiker[2]

Department of Chemical Engineering and Industrial Chemistry, Swiss Federal Institute of Technology, ETH-Zentrum, Zürich CH-8092, Switzerland

Received October 25, 1994; in revised form March 6, 1995; accepted March 8, 1995

The products of the decomposition of chromium(III) nitrate nonahydrate (CNN) and interconversions occurring in the system CrO_2–CrOOH have been investigated using thermal analysis, mass spectrometry, X-ray powder diffraction, and magnetic resonance. The studies indicate that changes in the conditions of CNN calcination, especially in the temperature, greatly influence the ratio of Cr(IV) to Cr(III) oxides in the products. CrO_2 formed during slow heating to ca. 350°C is very stable and its complete transformation into Cr_2O_3 requires a temperature higher than 600°C. The rapid crystallization of the amorphous products of CNN calcination, occurring at ca. 380°C, leads to the decomposition of all intermediates during this strongly exothermal reaction, finally resulting in Cr_2O_3. The interconvertability of the components of the redox cycle CrO_2–CrOOH was proven experimentally. Due to its unique characteristics, this redox cycle is suggested for the difficult identification of CrO_2 in amorphous chromium–oxygen systems. © 1995 Academic Press, Inc.

INTRODUCTION

The decomposition of chromium(III) nitrate nonahydrate (CNN) ($Cr(NO_3)_3 \cdot 9H_2O$) deposited on an oxide carrier is commonly used as a method for the preparation of supported chromium oxide catalysts. CNN decomposition is characterized by the formation of a liquid phase at low temperatures (below 70°C) followed by the formation of an amorphous foam-like solid. Further heating leads to violent crystallization concomitant with the decomposition of the previously existing intermediates. Depending on the applied atmosphere, temperature, heating rate, and time of decomposition, different products can be formed. Temperatures as high as 600–700°C can be necessary for total conversion into Cr_2O_3. The use of such high temperatures for the calcination of the catalyst precursors can cause drastic changes in the surface area, porosity, and microstructure, which in turn influence the catalytic behavior of the catalyst.

Disagreement exists in the literature (1–9) regarding the formation of chromium dioxide, CrO_2, as an intermediate or product of CNN decomposition. The existence of CrO_2 has been mentioned in a few reports (1, 3, 6); however, only Fouad *et al.* (3) confirmed their conclusions by presenting experimental data. Although the particular reactions occurring in the system CrO_2–CrOOH have been studied in the literature (reduction of CrO_2 in (10–15) and oxidation of CrOOH in (15–18)), the complete, reversible cycle $CrO_2 \rightleftharpoons$ CrOOH has not been investigated yet.

The lack in the understanding of the complex structural and chemical changes occurring during CNN decomposition prompted us to investigate this reaction and the related interconversions of relevant chromium oxide phases using thermogravimetry (TG), differential thermal analysis (DTA), mass spectrometry (MS), X-ray powder diffraction (XRD), and magnetic resonance measurements. Magnetic resonance was found to be a suitable tool for the qualitative identification of several chromium oxide phases because of their distinct magnetic properties: CrO_2 is ferromagnetic below its Curie temperature T_c (ca. 120°C), a property never established for any other chromium oxides. CrOOH and Cr_2O_3 are typical antiferromagnetic materials with Néel points T_N of ca. −150°C (19) and 35°C (20), respectively.

The detailed knowledge of CNN decomposition and interconversion reactions of the relevant chromium oxide phases (CrO_2, CrOOH, and Cr_2O_3) reported in this work should provide the scientific basis for the preparation of the supported chromium oxide phases with well-defined composition.

EXPERIMENTAL

The investigations were performed with either single phases (CrO_2 and CrOOH) or multicomponent samples obtained by the decomposition of CNN (p.a., Fluka).

[1] Present address: Fritz Haber Institute, Max Plank Society, D-14195 Berlin, Germay.

[2] To whom correspondence should be addressed.

0022-4596/95 $12.00

CrO_2 manufactured by Aithaca Chemical Corp. (USA) was heated in air at 400°C prior to further use, in order to decompose the CrOOH present in the sample and to remove the organic impurities (weight loss due to the presence of these phases was in the range of 2.3 wt.%).

CrOOH was prepared by the reduction of the chromium dioxide with pure hydrogen (containing less than 0.005 vol.% of impurities) heating with a rate of 10 K/min in the range 25–350°C. XRD analysis made after this preparation procedure confirmed the presence of one phase only, showing a diffraction pattern identical to that of guyanite–CrOOH (JCPDS file 20-0312). CNN was heated using a temperature ramp as applied for the preparation of chromia-containing catalysts (21), the black foam obtained from CNN decomposition at 225°C (21 hr) was heated 3 hr in oxygen at 300°C.

The decomposition of CrO_2 or CrOOH was investigated in pure argon (less than 0.005 vol.% of impurities), and their reactions with 6 vol.% H_2 were carried out on a thermobalance or in a specially constructed microreactor.

Thermoanalytical measurements were performed with a heating rate of 10 K/min on either a Mettler 2000C thermoanalyzer or a Netzsch STA 409, with α-alumina as a reference. Evolving gases were monitored on-line using a Balzers QMG 420 quadrupole mass spectrometer connected to the thermoanalyzer by a heated capillary.

X-ray analysis was carried out on a Siemens D5000 powder X-ray diffractometer using CuKα radiation in step mode between 20 and 80° 2θ, with a step size 0.01° and 0.3 sec.

The amount of oxygen contained in the samples was measured by mass spectrometric (Balzers GAM 455) determination of O_2 which evolved during heating the material in a fused-quartz microreactor with a heating rate of 10 K/min in helium flow (300 ml/min STP).

Paramagnetic, ferromagnetic, and antiferromagnetic resonance spectra were recorded on a Bruker ESP300 system at X-band frequency (Varian E-9 spectrometer at Q-band frequency), at temperatures between 77 (130) and 420 (300) K, microwave frequency about 9.5 (35.5) GHz, microwave power $\leq$1 mW, and modulation frequency 100 kHz. The numbers in parentheses refer to Q-band measurements. The measurements were carried out in a Bruker TE104 double rectangular cavity and a modified Varian E-266 Q-band TE011 (right circular cylinder) cavity, respectively. The g values were determined with a NMR magnetometer and DPPH as g marker. The spectra intensity was obtained by numerical double integration of the sample and reference (DPPH) spectra using the ESP300 software.

RESULTS

Decomposition of CrO_2

Thermoanalytical (TA), mass spectroscopic (MS), and XRD results concerning the decomposition of chromium dioxide in argon are depicted in Fig. 1. The recorded weight loss (9.4%) agrees well with that which is expected from the stoichiometry of the decomposition of CrO_2 to Cr_2O_3 (9.52%). The XRD patterns of the reactant taken before the decomposition (sample 1 in Fig. 1) were fully consistent with the JCPDS file 9-332, indicating that the CrO_2 used did not contain any other phase, at least not in an amount detectable by XRD. The decomposition starts at about 360°C and shows two endothermal peaks at 467 and 510°C, respectively. It proceeds in two discernible steps; the first step, corresponding to CrO_2 conversion up to 0.85 (conversion $\alpha = 1$ corresponds to total decomposition to Cr_2O_3), occurs in the range 360–590°C. The completion of the reaction requires temperatures as high as 820–850°C. XRD analysis of the decomposition product (sample 2 in Fig. 1) confirmed the presence of Cr_2O_3. The amount of evolved oxygen determined by MS was 9.6%, confirming the high purity of the chromium dioxide used.

Redox Cycle $CrO_2 \rightleftharpoons$ CrOOH

The distinct decrease of the rate of CrO_2 reduction at higher conversion (0.80–0.85) (11–13) and the possible decomposition of the reduction obtained at higher temperature require a careful examination of the yield of the interconversion reactions occurring in the system $CrO_2 \rightleftharpoons$ CrOOH. Figure 2 summarizes the interconversions occurring, as revealed by TA and XRD.

CrOOH was prepared from chromium dioxide by heating to 390°C in a pure hydrogen atmosphere with a rate

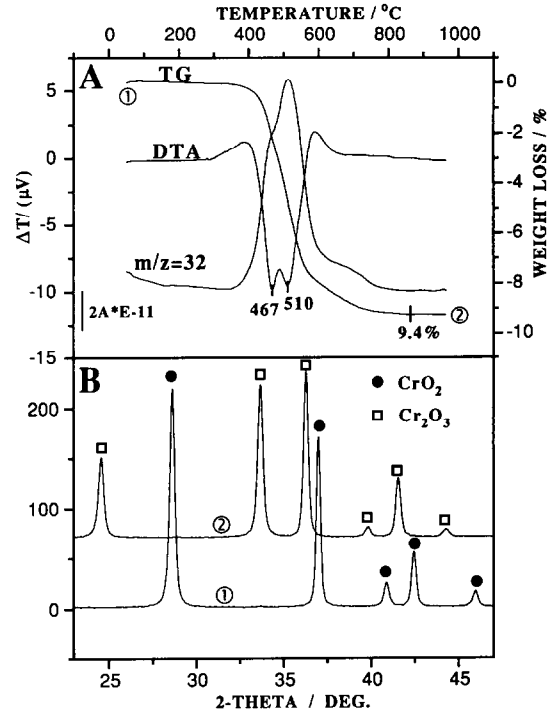

FIG. 1. Decomposition of CrO_2 in argon studied by TG, DTA, and MS.

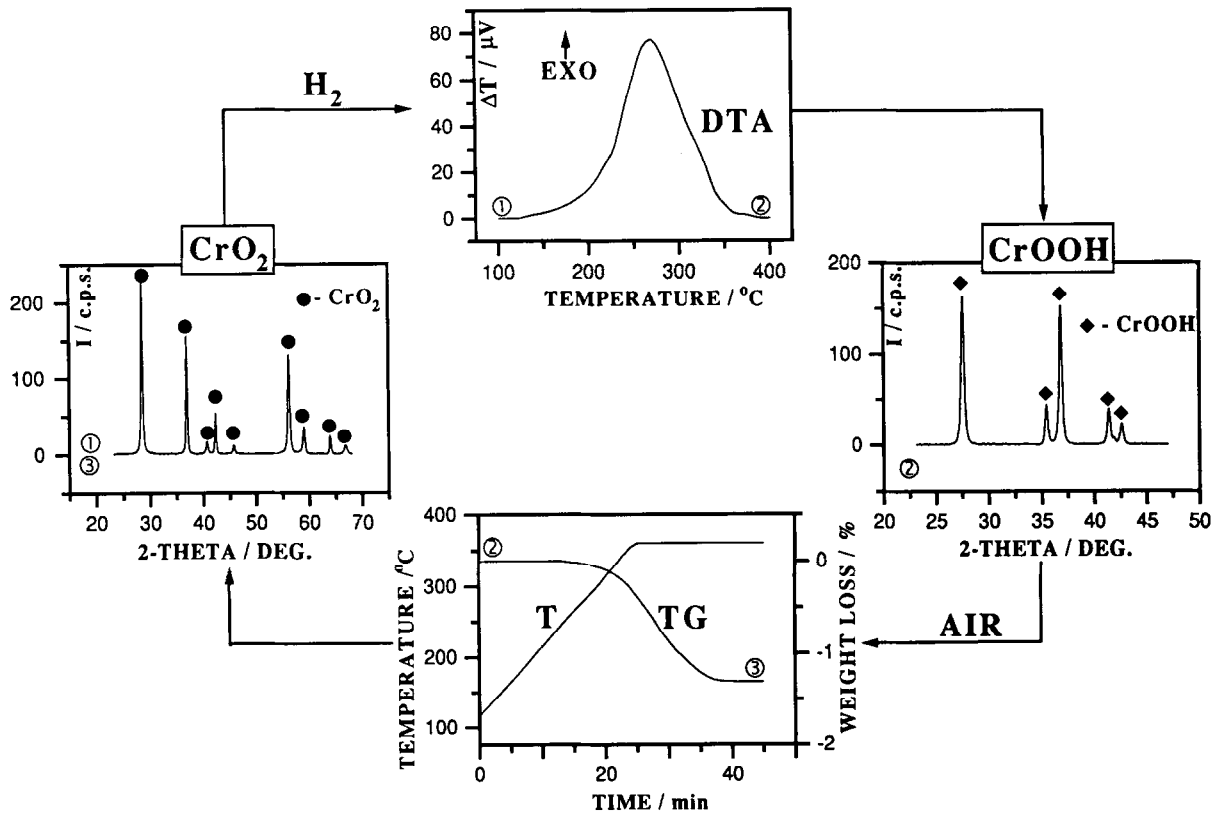

FIG. 2. Interconversions occurring under different conditions in the system $CrO_2 \rightleftharpoons$ CrOOH. XRD patterns correspond to samples taken at points 1, 2, and 3 labeled on the thermoanalytical curves. CrO_2 was heated under hydrogen (with heating rate 10 K/min) to 390°C. The CrOOH formed was transformed to CrO_2 by isothermal heating in air at 360°C.

of 10 K/min. The DTA curve indicates that the exothermal reduction of Cr(IV) to Cr(III) occurs in the range 125–385°C with the maximum at 270°C. The XRD patterns of the reduction product taken after heating to 390°C (point 2 on DTA curve) were identical to the data of the guyanite–CrOOH. No other phases were detected by XRD.

The CrOOH formed was oxidized in air by heating it to 360°C with a rate of 10 K/min and maintaining this temperature for about 25 min until constant weight was reached (TG curve in Fig. 2). The observed weight loss (1.3%) corresponds well to that expected from stoichiometry (1.2%) for the transformation of CrOOH $\rightarrow$ CrO_2. The XRD patterns for the sample, taken at point 3 on the TG curve (after completion of the oxidation reaction), were identical to those measured before the reduction–oxidation cycle and characteristic for CrO_2.

The results presented in Fig. 2 confirm that under the experimental conditions applied, a reversible interconversion $CrO_2 \rightleftharpoons$ CrOOH is possible. This was confirmed by the decomposition of CrO_2 in argon after one redox cycle. The corresponding thermoanalytical curves showed the same temperature dependence as those measured before the first redox cycle (Fig. 1).

Decomposition and Reactivity of CrOOH

In argon CrOOH starts to decompose at about 320°C under the conditions used, as illustrated in Fig. 3. The maximum rate of water evolution occurs at 567°C and the reaction ceases at ca. 790°C. The DTA curve of the endothermal decomposition of CrOOH shows two maxima centered at 418 and 557°C. The weight loss of 10.0% is smaller than that expected from stoichiometry (10.59%) for the decomposition of CrOOH $\rightarrow$ Cr_2O_3. MS curves presented in Fig. 3B indicated that H_2O is the main gaseous product of CrOOH decomposition, but smaller amounts (note sensitivity of respective m/z curves) of hydrogen and oxygen are also detectable. XRD indicated that the product of the decomposition (point 2 on the TG curve) contained only eskolaite–Cr_2O_3 (JCPDS file 38-1479).

The decomposition of CrOOH in hydrogen (6 vol.% H_2 in Ar) is shifted to higher temperatures, and evolution of water occurs in the range 355–900°C. Figure 4 illustrates the decomposition in air, which starts at significantly lower temperatures (ca. 265°C). The mass spectrometric results indicate that decomposition is initially accompanied by oxygen consumption and production of water and

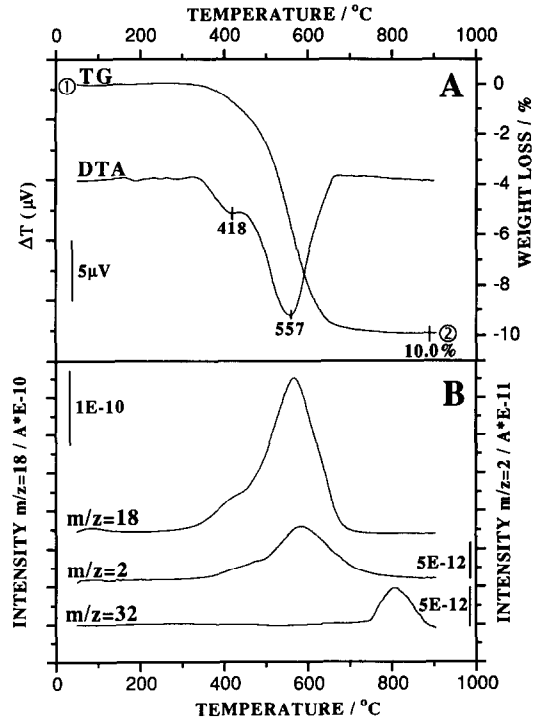

FIG. 3. Decomposition of CrOOH (synthesized from CrO_2 by reduction with hydrogen) in inert atmosphere (argon). (A) Thermoanalytical and (B) mass spectrometric (m/z = 2, 18, and 32) results.

later by oxygen evolution. XRD analysis indicated that the product contained only Cr_2O_3.

Characterization and Reactivity of CNN Decomposition Products

The thermoanalytical and X-ray diffraction results of CNN decomposition products obtained under conditions comparable to those used in catalyst preparation (21) are presented in Fig. 5. The TG curve shows a weight loss in the range 340–955°C caused by oxygen evolution (m/z = 32 curve). The XRD data (Fig. 5B) indicate that the solid is made up of two phases: Cr_2O_3 and CrO_2. After thermal analysis (point 2 on TG curve) only Cr_2O_3 is present. The completion of CrO_2 decomposition (ca. 950°C) is shifted by more than 100° to higher temperatures compared to the pure oxide. From the observed weight loss we estimate that the CrO_2 content amounts to ca. 37 wt.% of the CNN decomposition products.

Mass spectrometric determination of the amount of evolved oxygen indicates that under the conditions used for the preparation of supported catalysts the amount of CrO_2 contained in the products of chromium nitrate decomposition is 37.6 wt.%.

Heating the CNN decomposition products in argon after the cycle $CrO_2 \rightarrow CrOOH \rightarrow CrO_2$ is depicted in

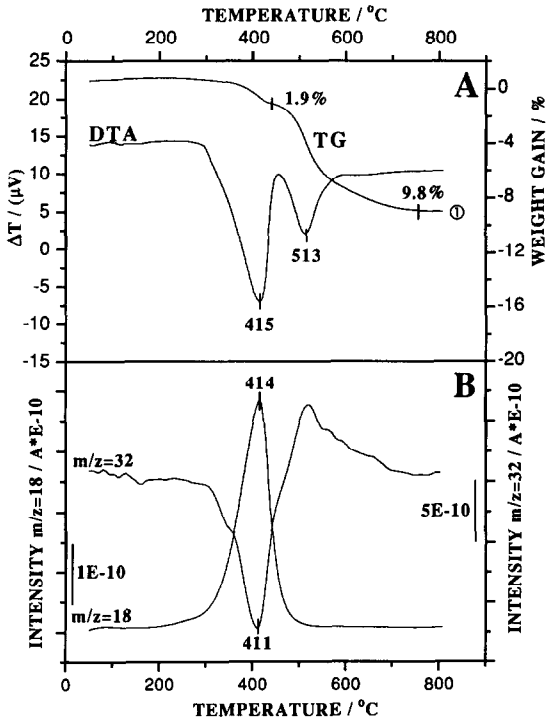

FIG. 4. Decomposition of CrOOH in oxidizing atmosphere (air). (A) Thermoanalytical and (B) mass spectrometric (m/z = 18 and 32) results.

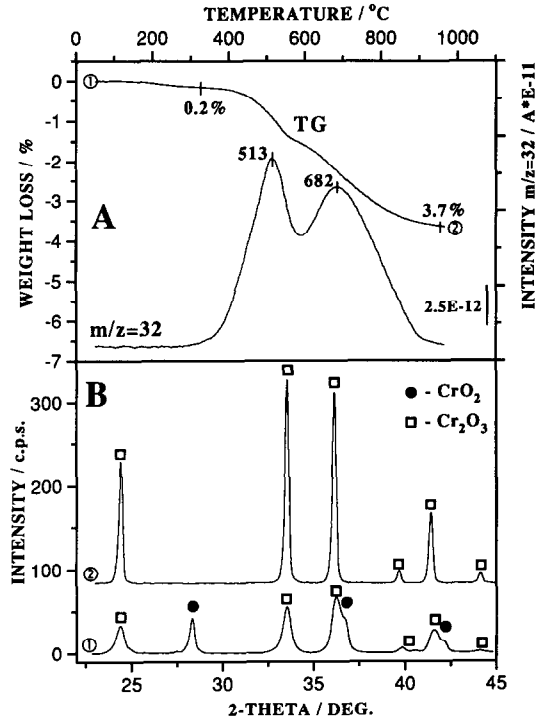

FIG. 5. Decomposition of the products of CNN calcination (225°C, 21 hr, air followed by 300°C, 3 hr, oxygen) in argon: (A) Mass spectrometric (m/z = 32) and thermoanalytical results. (B) XRD patterns of the samples (1) before and (2) after thermal treatment.

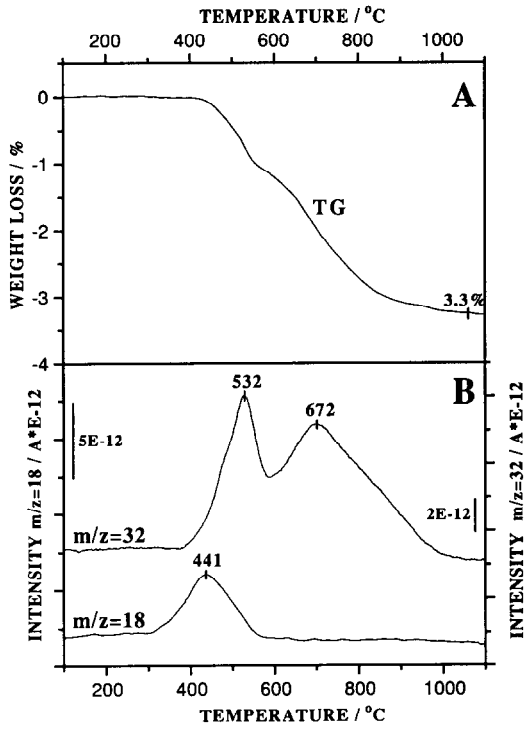

FIG. 6. Decomposition in argon of the products of CNN (225°C, 21 hr, air followed by 300°C, 3 hr oxygen) calcination after their reaction with hydrogen followed by oxidation in air. (A) Thermoanalytical and (B) mass spectrometric (m/z = 18 and 32) results.

Fig. 6. As for pure CrO_2, the measured weight loss is a little smaller than that measured for the "parent" solid before the cycle. The residual water which evolved in the range 300–580°C indicates that a small part of CrOOH was not completely transformed to CrO_2 during the second step of the redox cycle. The maxima on the mass spectrometric curve indicate that the oxygen evolution occurs almost at the same temperatures as for the original solid (before cycle), cf. Figs. 5 and 6. Only completion of the decomposition is shifted to higher temperatures (from 950 to 1070°C) for the sample after the redox cycle.

The results concerning the products of CNN calcination, presented above, were obtained for the solid, which after 21 hr decomposition at 225°C was additionally calcined in oxygen for 3 hr at 300°C. In order to examine the composition of the product of CNN calcination at 225°C and to draw conclusions concerning the influence of the second calcination step (300°C, oxygen), the product after the first calcination were analyzed. The analysis was obscured by the fact that the sample was an amorphous and black solid. Neither infrared spectroscopy nor XRD provided conclusive results and the magnetic resonance spectra did not allow a clear distinction between paramagnetism and superparamagnetism, i.e., between Cr(III) and CrO_2.

TA and MS curves of the CNN calcination product (225°C, 21 hr, air) heated in argon are shown in Fig. 7. The mass spectroscopic curve m/z = 30 indicates that the evolution of the residual NO, being present in the solid, begins at ca. 200°C. Water evolved in three steps: the first step (25–200°C) was due to weakly adsorbed water (TG curve shows weight loss of 1.2 wt%); the second step, where the main part of H_2O was released, occurred in the range 210–370°C; the third step was accompanied by crystallization, occurring in the range 370–390°C. The evolution of oxygen started at 310–315°C and was complete at 430°C. The main part of oxygen is released during a very rapid, strongly exothermal crystallization, with a maximum at 382°C (DTA curve in Fig. 7). The rapid, explosion-like decomposition could be monitored only by reducing the heating rate from 10 to 2 K/min. The XRD patterns of the products taken at 480°C indicated the presence of Cr_2O_3 only.

Observed evolution of NO (ca. 10% of the amount of evolved water) in the range 210–370°C can be explained by the decomposition of the basic chromium nitrates, bichromates, and chromates as has been postulated in Ref. (2). In order to remove these species and to improve the reliability of the analysis of the oxygen evolution accompanying the main decomposition reactions, the products of CNN calcination, described above, were additionally heated in argon for 3 hr at 300°C. XRD analysis

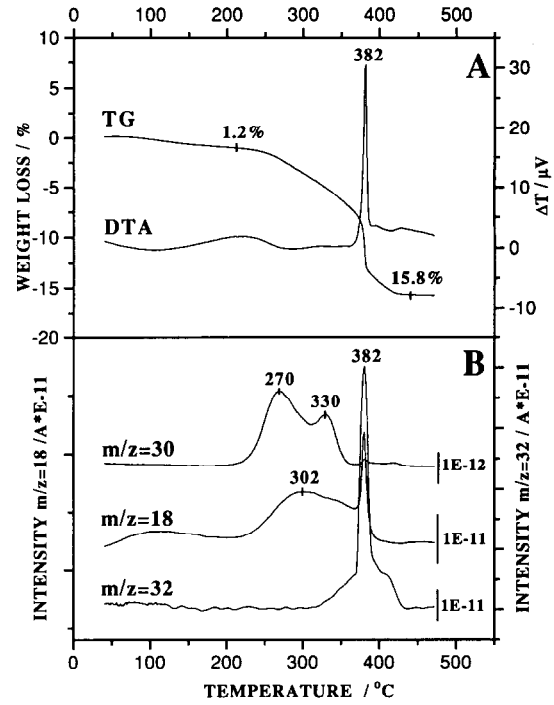

FIG. 7. Decomposition in argon of the products of CNN calcination at low temperature (225°C, 21 hr, air). (A) Thermoanalytical and (B) mass spectrometric results.

showed that after this heat treatment the solid was still amorphous. The corresponding DTA and MS results (evolution of water and oxygen) are presented as curves A in Fig. 8. The observed evolution of oxygen can be interpreted as the result of CrO_2 decomposition. The characteristic redox cycle $CrO_2 \rightleftharpoons CrOOH$ was used for the identification of the chromium dioxide, because only this oxide among all other chromium–oxygen containing compounds can be reoxidized after reduction by hydrogen.

To confirm this, the CNN calcination products (225°C, 21 hr, air, followed by 300°, 3 hr, argon) were heated in hydrogen (250°C, 1 hr) and then reoxidized by oxygen at 300°C for 3 hr. The corresponding DTA and MS curves (m/z = 18 and 32) monitored for the decomposition of sample B (sample A after reduction) and sample C (sample B after reoxidation) are shown in Fig. 8. They indicate that after reaction with H_2 the sample contained about 20% of the original amount of oxygen. The amount of water which evolved during the second stage, i.e., between 200–430°C, was more than seven times larger than that for the sample before reduction. Due to the "mild" conditions compared to those applied with the corresponding crystalline solids, the solid–gas reactions were not complete, as indicated by the presence of the small

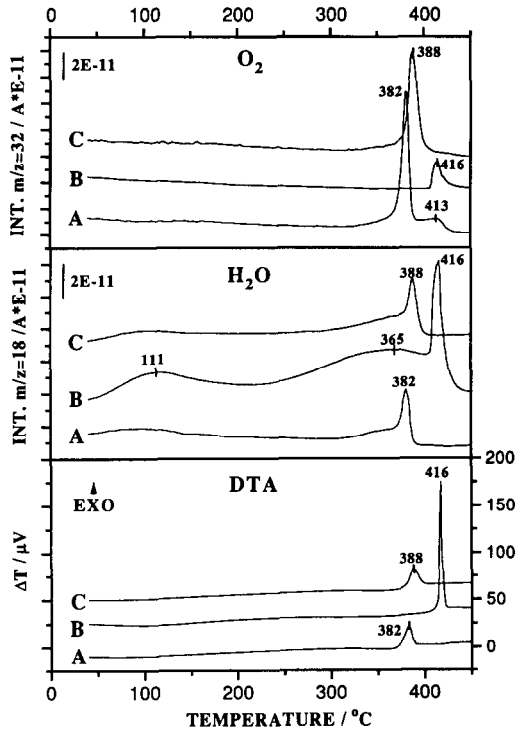

FIG. 8. Mass spectrometric (m/z = 32 and 18) and DTA curves of the decomposition in argon of the products of CNN calcination (225°C, 21 hr, air followed by 300°C, 3 hr, argon) after subjecting the samples to different treatments: (A) as received, (B) sample A after reaction with hydrogen (250°C, 1 hr), and (C) sample B after reoxidation by oxygen (300°C, 3 hr).

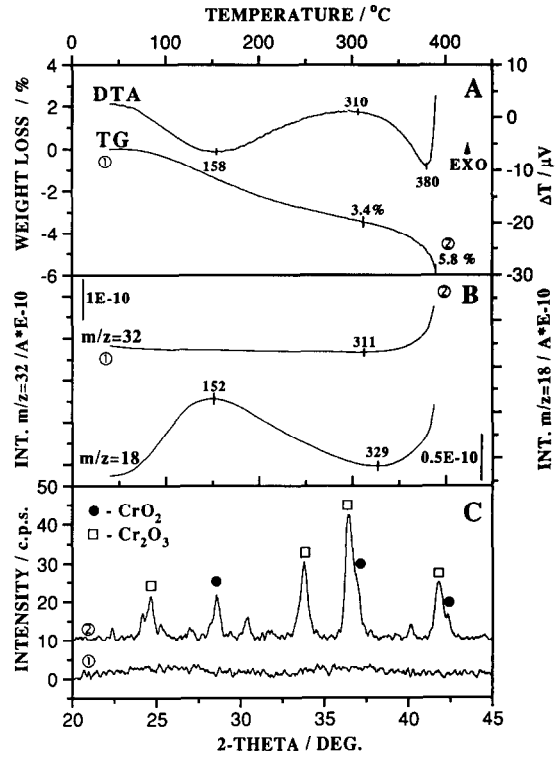

FIG. 9. (A) Thermoanalytical, (B) mass spectrometric, and (C) XRD results of the product of CNN calcination (225°C, 21 hr, air followed by 300°C, 3 hr, argon) heated in argon to 388°C.

amount of the reactants after the particular redox stages. After reoxidation (curves C in Fig. 8) the mass spectrometric and DTA curves were similar to curves A, measured before the redox cycle.

The DTA curves indicate the differences in the crystallization of the amorphous solids in particular stages of the redox cycle. For the parent material (sample A) and product of the redox reactions (C), the temperatures of crystallization are similar (382 and 388°C, respectively). The crystallization of the amorphous product after reduction (sample B) occurs at higher temperature (416°C) and is more rapid than that of samples A and C.

The results presented above confirm the occurrence of the CrO_2 in the amorphous products obtained by low temperature calcination of CNN. As previously mentioned, the redox cycle is specific for this compound. For a direct proof the following experiment was carried out (Fig. 9). The sample already heated in argon at 300°C (sample A in Fig. 8) was heated in a thermobalance to the temperature at which the solid started to crystallize (388°C). At this temperature evolution of oxygen had already occurred, but the TG and DTA (Fig. 9A) and MS (Fig. 9B) curves showed that not more than 20% of CrO_2 present in the sample was decomposed. This determination was made by comparison of the weight loss and amount of evolved oxygen at 388°C with the results ob-

tained during total decomposition (heating to 470°C, data not presented). At 388°C the sample was quenched and subjected to XRD analysis. The sample before this experiment was X-ray amorphous, and the one taken at 388°C was made up of poorly crystalline phases of CrO_2 and Cr_2O_3, as indicated by the XRD patterns shown in Fig. 9C.

Magnetic Measurements

The magnetic resonance spectra (ν = 9.5 GHz) of the products of CNN calcination (Ar, 225°C plus O_2, 300°C) are shown in Fig. 10A for different recording temperatures. The spectral patterns depend strongly on temperature with respect to width (ΔB_{pp}), intensity (numerical double integral), g value, and the shape of the lines. Above 125°C, i.e., approximately at the Curie temperature of CrO_2, a symmetric derivative line is observed for T = 125°C with g = 1.97 and ΔB_{pp} = 40 mT, and for T = 147°C with g = 1.96 and ΔB_{pp} = 18 mT. Below 125°C, the line width is considerably broadened with decreasing temperature—at 100° ΔB_{pp} = 160 mT (Fig. 11B)—and the line becomes asymmetric. As shown in Fig. 11A, the intensity (double integral) of the spectrum notably increases in the

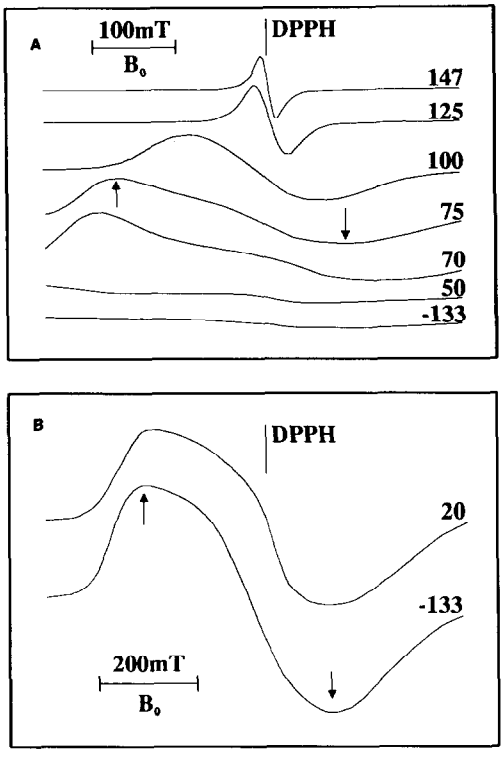

FIG. 10. Magnetic resonance spectra of the product of CNN calcination (225°C, 21 hr, air followed by 300°C, 3 hr, oxygen) for different recording temperatures (A) at X-band (ν = 9.5 GHz) and (B) at Q-band (ν = 35.5 GHz). The arrows indicate where the ΔB_{pp} values were taken from the spectra. Note that, although not seen from the diagrams because of a problem in scale, the sample had a remarkable magnetic moment even below room temperature.

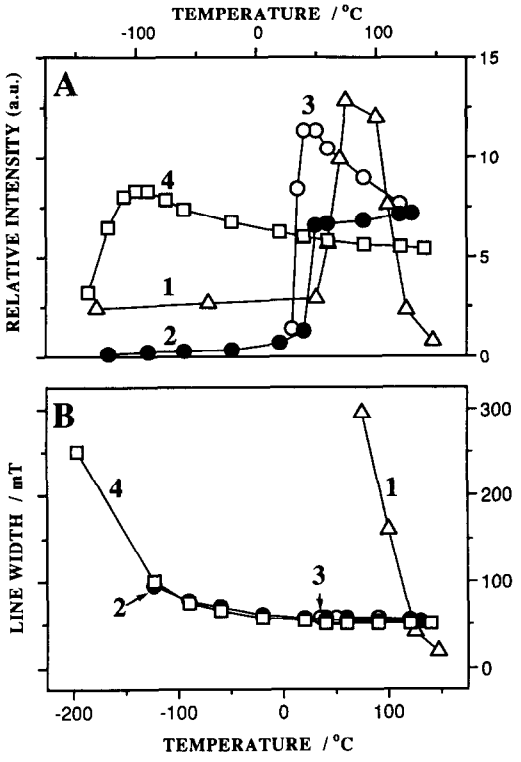

FIG. 11. Temperature dependence (A) of the magnetic resonance spectra intensity (thermomagnetic curves) and (B) of the line widths (ΔB_{pp}, peak to peak) for the following samples: (1) product of CNN calcination (225°C, 21 hr, air followed by 300°C, 3 hr, oxygen), (2) sample 1 after reduction by hydrogen (10 K/min to 390°C), (3) sample 1 after decomposition in argon at 950°C, and (4) pure CrOOH prepared from CrO_2 by reduction (10 K/min to 390°C, hydrogen). The relative intensity curves are shifted for better clarity and their absolute values are not comparable to one another.

range 125–75°C, but below 75°C it decreases abruptly to a finite value, which is still much larger than expected for a paramagnetic system. Note that the curves for the different chromium oxide phases in Fig. 11A are shifted for better representation and that the intensity obtained represents an approximation and is expected to be too small for the lower temperatures because of its uncertainty in the zero field region (22). The line broadening is accompanied by the appearance and low-field shift of a low-field shoulder (line width $\Delta B_{1/2}$ = 80 mT). This shoulder (absorption peak) extends to zero field at temperatures below 50°C at X-band frequencies. At the frequency of 35.55 GHz it appears at 1.03 Tesla as an asymmetry of a broad derivative line with ΔB_{pp} = 400 mT and g = 2.00 between 20°C and −133°C.

The magnetic resonance spectra described above show similarities to those of mixed chromium oxides CrO_x (x = 2.0–2.6) reported by Rode *et al.* (23). They show simultaneously the typical collective magnetic properties of an antiferromagnetic and a ferromagnetic system. The

abrupt decrease of the signal intensities at the Néel temperature T_N = 35°C of Cr_2O_3 is expected for this antiferromagnetic compound (20). The g shift, the great line widths and line asymmetry, and the large magnetization of the materials are proofs for ferromagnetism. The temperature dependence of the line asymmetry (low-field shoulder) is due to magnetic anisotropies of ferromagnetic CrO_2 (24). In reference to the literature, the magnetic anisotropies of CrO_2 could be expected to be due to a shape and a magnetocrystalline and magnetostriction component. On the other hand, according to Meiklejohn (25), the interaction between an antiferromagnetic substance and a ferromagnetic one below the Néel temperature results in a strong exchange anisotropy for systems with $T_N < T_c$, which also is valid for the system Cr_2O_3–CrO_2. When the antiferromagnetic substance turns into a paramagnetic one above T_N, the magnetic behaviors are dominated by the ferromagnetic component. Similar magnetic behavior was reported, e.g., for the system cobalt–cobalt oxide (26) and platinum–Cr_2O_3 (27). We can deduce that the CNN calcination product represents a mixture of an antiferromagnetic and a ferromagnetic, which is in agreement with the XRD and thermoanalytical results.

After decomposition of the CNN calcination product in argon at 955°C (cf. Fig. 5, point 2 on TG curve), the magnetic resonance spectra are typical for an antiferromagnetic system. The resonance line is symmetric with g = 1.98 and ΔB_{pp} = ca. 55 mT. The temperature dependence of the line width and intensity is given in Fig. 11, curve 3. The intensity decreases abruptly below about 37°C, which agrees well with the Néel point T_N of Cr_2O_3, according to (20) T_N = 35°C. A few degrees below T_N the absorption disappears completely. The same behavior was found for pure Cr_2O_3 prepared by the thermal decomposition of crystalline chromium dioxide (sample 2, see TG curve, Fig. 1).

The magnetic properties of CrOOH prepared from bulk CrO_2 by its reduction with hydrogen (sample 2 in Fig. 2) are presented in Fig. 11, curve 4. The figure depicts the temperature dependence of the intensity and line width of the corresponding symmetric derivative line at g = 1.98. The behavior observed below − 113°C is typical antiferromagnetic, as expected for β-CrOOH, although this temperature is about 40° higher than the Néel point for β-CrOOH given in the literature (19).

The reduction of the CNN calcination products by hydrogen yields a solid having magnetic properties "intermediate" between Cr_2O_3 and CrOOH, see curves 2 in Fig. 11. An abrupt decrease of the antiferromagnetic resonance signal is observed at about 47°C, similar to Cr_2O_3 (35°C), but a finite signal intensity remains below this temperature due to the presence of CrOOH. The line widths are intermediate between Cr_2O_3 and CrOOH and their temperature dependence is analogous to CrOOH. The magnetic behavior of pure Cr_2O_3 (28, 29) and β-CrOOH (19) is well documented in the literature.

The ferromagnetic resonance spectra of the sample prepared by CNN decomposition (225°C, air, 21 hr followed by 300°C, argon, 3 hr) and quenched at 388°C during heating in argon with 2 K/min (compare also Fig. 9) prove the presence of CrO_2 (in addition to Cr_2O_3). The strong magnetic moment and the temperature dependence of the line widths and intensities (not shown) resemble those of the crystalline mixture of CrO_2 and Cr_2O_3 obtained by calcination in oxygen at 300°C and described above. Due to the particle size and measurement time, the system has to be regarded as ferromagnetic rather than superparamagnetic (30).

DISCUSSION

The chemistry of the solid products of CNN decomposition is complex due to the multivalence of chromium and investigations are rendered difficult by the occurrence of poorly crystalline products. Discrepancies are most obvious with regard to the formation of CrO_2 during decomposition.

In order to gain information about the phase composition of CNN calcination products, we have tested the reactivity of all chromia phases, possibly involved in the decomposition, in the reducing and oxidizing atmospheres and have measured their magnetic properties. This strategy has been chosen due to the unique properties of CrO_2: strong ferromagnetic behavior and reversible reducibility to Cr(III).

Chromium dioxide decomposes in an inert atmosphere into Cr_2O_3 over a wide temperature range. The course of the thermoanalytical curves presented in Fig. 1 indicates that temperatures higher than 800°C are necessary for total conversion of CrO_2. The low rate of oxygen evolution above 600°C suggests that, even under isothermal conditions, complete transformation into Cr_2O_3 will require temperatures higher than 550–600°C. The shape of the oxygen evolution curve and DTA curve (Fig. 1) confirm the suggestion of Alario-Franco *et al.* (31) that decomposition of CrO_2 proceeds through intermediate chromium oxides.

Our results concerning the CrO_2 decomposition, in argon and air, do not support the conclusion of Fouad *et al.* (3) that during heating CrO_2 disproportionates into Cr_2O_3 and CrO_3. Such a disproportionation, if possible at all, could occur only below 200°C, because at higher temperatures CrO_3 is not stable (after melting at 197°C (32); it starts to decompose, forming chromium oxides Cr_3O_8, Cr_2O_5, CrO_2, and finally Cr_2O_3 (33–36)). Other literature data concerning CrO_2 decomposition (10, 31, 34, 37–42) also exclude the disproportionation during the course of reaction. In addition, the statement concerning

the oxidation of Cr^{+3} to Cr^{+6} presented in (3) and (43, 44) seems to need further discussion. Literature data dealing with the decomposition of CrO_3 (33–36) univocally indicate that in the system CrO_3–Cr_2O_3 only reduction of the chromium oxidation state occurs under atmospheric pressure (from chromium(VI) oxide via bivalent Cr (VI, III) oxides and Cr(IV) dioxide to Cr(III) oxide). The statement concerning the oxidation of Cr^{+3} to Cr^{+6} made in (44) has not been experimentally proven by the authors.

All chromium oxides (except CrO_2) containing chromium with a valence higher than +3, i.e., Cr(VI) oxide or Cr_2O_5 (which, as has been reported in (45), is a Cr^{3+}/Cr^{6+} mixed-valence compound with the composition $Cr_2^{3+}Cr_4^{6+}O_{15}$), are reduced irreversibly by hydrogen to chromium(III) oxide. Cr_2O_3 can be reduced by hydrogen only at a very high temperature; even at 1310°C the partial pressure of water is very low, in the range of 1.5 mbar (46). The only exception is the reduction of CrO_2 with hydrogen, yielding β-CrOOH, which in turn can be oxidized to chromium(IV) dioxide.

Discussing the problem of the interconversion in the system CrO_2-CrOOH, it is necessary to take into account the problem of the thermal stability of both compounds, which decompose irreversibly to Cr_2O_3 at higher temperatures. The data illustrating the cycle CrO_2–CrOOH–CrO_2 (Fig. 2) confirm that, under carefully chosen experimental conditions, this interconversion is possible with a yield as large as 95%. The presence of the residues of the unreacted "parent" solids, i.e., CrO_2 for the reduction and CrOOH for the reoxidation, is not detectable by XRD.

Studying the interconversion occurring in the system $CrO_2 \rightleftharpoons$ CrOOH required the investigation of the stability and course of the decomposition of chromium oxy-hydroxide. Decomposition of CrOOH can occur in two ways:

$$2CrOOH \rightarrow 2CrO_2 + H_2 \qquad [1a]$$

$$2CrO_2 \rightarrow Cr_2O_3 + \tfrac{1}{2}O_2 \qquad [1b]$$

or

$$2CrOOH \rightarrow Cr_2O_3 + H_2O. \qquad [2]$$

The shift of the decomposition up to higher temperatures in hydrogen seems to confirm mechanism [1a]. Decomposition in air (Fig. 4) indicates, however, that the reaction passes through two stages: (i) oxidation of the reactant to CrO_2, followed by (ii) chromium dioxide decomposition. The beginning of the weight loss is indicated on the TG curve at ca. 260°C. The mass spectrometric curve $m/z = 32$ shows the beginning of the oxygen consumption at about 270°C, which, together with the course of the water evolution curves ($m/z = 18$) and the observed shift of the reaction to lower temperature, supports the decomposition stage [1a]. Note that water evolved in the same temperature range in which consumption of oxygen occurred. After completion of stage [1a], stage [1b] starts to dominate the course of the reaction, as indicated by the evolution of oxygen occurring until about 750°C and by the change of the mass recorded by TG. Results presented in Fig. 3 indicate that in Ar mechanism [2] seems to be decisive (see H_2O evolution), but part of CrOOH is also decomposed via route [1a]—note H_2 evolution. The influence of the decomposition atmosphere explains the difference in the results reported in Refs. (10) and (13).

The thermoanalytical data presented in Figs. 5 and 6, as well as the magnetic resonance studies, clearly confirm the presence of CrO_2 in the products forming on CNN calcination at 300°C. These products are poorly crystalline (curve 1 in Fig. 5B); nevertheless, the XRD patterns of Cr_2O_3 and CrO_2 are apparent. The measured weight loss (TG curve, Fig. 6A) and the amount of oxygen which evolved indicate a CrO_2 content of ca. 37 wt.%. The investigations of the interconversion cycle for CNN calcination products (Fig. 9) confirm (i) its quantitative composition and (ii) that the reactivity of the solids formed is similar to that observed for the corresponding pure bulk phases. The yield of the conversion CrO_2–CrOOH–CrO_2 is ca. 94%, as a comparison of the weight loss caused by CrO_2 decomposition before (3.5%, Fig. 5) and after the conversion cycle (3.3%, Fig. 6) reveals.

The magnetic resonance data of the products of CNN calcination are in absolute agreement with the results of XRD and thermal analysis for all experiments performed. Chromium dioxide is the only known transition metal oxide which is ferromagnetic at room temperature. This property can serve as the specific identification in pure chromium oxide systems and in the redox cycle $CrO_2 \rightleftharpoons$ CrOOH. There is no doubt that the ferromagnetism observed after particular treatment is due to CrO_2. The only restriction is that the particle size is too small to exhibit collective magnetic properties, as in the case of the products of CNN decomposition at 225°C. In this case, the application of the redox cycle, characteristic of the system $CrO_2 \rightleftharpoons$ CrOOH, can help in the interpretation of the phenomena occurring during the CNN decomposition.

The thermoanalytical investigations of the products of CNN calcination (heated only at 225°C) presented in Fig. 7 show that the removal of nitrogen compounds is not complete. The mass spectrometric curves seem to confirm the opinion of Gubrynowicz and Strömch (2), who suggested the presence of basic and normal chromium chromates and basic chromium nitrates (NO and H_2O represented by MS curves $m/z = 30$ and $m/z = 18$, respectively).

Gubrynowicz and Strömch (2) suggest that the violent

evolution of oxygen occurring above 300°C is caused by the decomposition of the bivalent(III, VI) chromium chromate $Cr_2(CrO_4)_3$. The proposed mechanism excludes the formation of a chromium oxide with the oxidation state Cr(IV), which is in contradiction to our results. The results presented in Fig. 8 clearly confirm the existence of CrO_2 in the amorphous products and the reversibility of the redox cycle $CrO_2 \rightleftharpoons CrOOH$.

The data presented in this work confirm the difficulty in determining CrO_2 after the violent crystallization of the amorphous CNN decomposition products. Amorphous CrO_2 begins to decompose around 300–310°C and a significant acceleration of this reaction occurs during the rapid crystallization. After crystallization only Cr_2O_3, the final product of all decomposition reactions occurring in the system, is present in the products.

The direct proof of the existence of CrO_2 in the CNN decomposition products is shown in Fig. 9. During very slow heating of the amorphous CNN decomposition products in argon (225°C, 21 hr, air followed by 300°C, 3 hr, Ar), partial crystallization occurred together with slow decomposition of CrO_2. After quenching the sample heated to 388°C, the XRD patterns (Fig. 9C) confirm the existence of two phases: CrO_2 and the product of its decomposition, Cr_2O_3. This result is further confirmed by the ferromagnetism of this sample.

The discrepancies found in the literature concerning the composition of CNN calcination products are understandable in the light of these results. During the heating, two processes occur simultaneously: decomposition of the amorphous CrO_2 and its crystallization, the latter accelerating the decomposition process. Depending on the rate of both processes, which are strongly influenced by the ambient atmosphere and temperature, the crystalline product possesses a different ratio of chromium(IV) to chromium(III) oxides. It is likely that this ratio is also influenced by the interaction of dispersed chromia with the support material of supported catalysts.

CONCLUSIONS

Magnetic resonance, thermoanalytical, and XRD investigations indicate the formation of chromium(IV) dioxide, CrO_2, as a stable product of the decomposition of chromium(III) nitrate nonahydrate. Changes in the conditions of CNN calcination, especially the atmosphere and the temperature, influence the ratio of Cr(IV) to Cr(III) oxides in the slowly crystallizing product. CrO_2 already formed decomposes at high temperatures and its complete transformation into Cr_2O_3 requires temperatures higher than 600°C, which are not commonly used in catalyst preparation. Because of the high thermal stability of CrO_2, its formation has to be taken into account when precursors such as CrO_3 or $Cr(OH)_3$ (33–36, 47) are used for catalyst preparation. Fast heating results in rapid crystallization (at ca. 380°C) of the fully amorphous products formed at low temperatures and finally results in Cr_2O_3 only, due to the decomposition of all intermediates during this violent, exothermal reaction.

The interconversion cycle $CrO_2 \rightleftharpoons CrOOH$ proceeds with a yield of ca. 95% under carefully chosen experimental conditions. The reversibility of this cycle was proven for pure reactants and for partially crystalline as well as fully amorphous solids and represents a characteristic feature aiding in the identification of CrO_2 in chromium–oxygen systems.

REFERENCES

1. G. C. Maiti, M. L. Kundu, and S. K. Ghosh, *J. Indian Chem. Soc.* **52,** 1119 (1975).
2. L. Gubrynowicz and T. Strömch, *Thermochim. Acta* **115,** 137 (1987).
3. N. E. Fouad, H. Knözinger, M. I. Zaki, and S. A. A. Mansour, *Z. Phys. Chem.* **171,** 96 (1991).
4. I. I. Kalinichenko, A. M. Sirina, and A. I. Purtov, *Russ. J. Inorg. Chem.* **19,** 843 (1974).
5. W. Wendlandt, *Tex. J. Sci.* **10,** 392 (1958).
6. W. D. Hill, Jr., *Inorg. Chim. Acta* **65,** L100 (1982).
7. J. Mu and D. D. Perlmutter, *Thermochim. Acta* **56,** 253 (1982).
8. A. M. Sirina, A. I. Purtov, I. I. Kalinichenko, and N. E. Konyukhova, *Russian J. Inorg. Chem.* **16,** 845 (1971).
9. A. W. Pamfilov, N. N. Puckova, and L. N. Kohanova, *Russian J. Inorg. Chem.* **1,** 2712 (1956).
10. M. A. Alario-Franco and K. S. W. Sing, *J. Therm. Anal.* **4,** 47 (1972).
11. R. Saez-Puche and M. A. Alario-Franco, *J. Solid State Chem.* **38,** 87 (1981).
12. R. Saez-Puche and M. A. Alario-Franco, *J. Solid State Chem.* **47,** 59 (1983).
13. R. Saez-Puche and M. A. Alario-Franco, *Thermochim. Acta* **74,** 273 (1984).
14. P. Porta, M. Marezio, J. P. Remeika, and P. C. Dernier, *Mater. Res. Bull.* **7,** 157 (1972).
15. N. C. Tombs, W. J. Croft, J. R. Carter, and J. Fitzgerald, *Inrog. Chem.* **3,** 1791 (1964).
16. Y. Shibasaki, *Mater. Res. Bull.* **7,** 1125 (1972).
17. S. Kitaka, T. Morooka, and K. Kitayama, *J. Solid State Chem.* **58,** 187 (1985).
18. K. Yabuta, N. Minomura, M. Shimada, F. Kanamaru, and M. Koizumi, *Mater. Res. Bull.* **13,** 1335 (1978).
19. A. N. Christensen, *Acta Chem. Scand. A* **30,** 133 (1976).
20. E. S. Dayhoff, *Phys. Rev.* **107,** 84 (1957).
21. K. Köhler, C. W. Schläpfer, A. Von Zelewsky, J. Nickl, J. Engweiler, and A. Baiker, *J. Catal.* **143,** 201 (1993).
22. M. Mörke, M. Hirschfelder, S. Gehre, and K. Doerffel, *Chemom. Intell. Lab. Syst.* **8,** 87 (1990).
23. T. V. Rode, V. B. Kazanski, and Yu. I. Pecherskaya, *Russ. J. Phys. Chem.* **35,** 2370 (1961).
24. V. Netzelmann, *J. Appl. Phys.* **68,** 1800 (1990).
25. W. H. Meiklejohn, *J. Appl. Phys.* **33,** 1328 (1962).
26. W. H. Meiklejohn and C. B. Bean, *Phys. Rev.* **105,** 904 (1957).
27. S. Engels, H. Lausch, B. Peplinski, M. Wilde, M. Mörke, and P. Kraak, *Appl. Catal.* **55,** 93 (1989).
28. L. R. Maxwell and T. R. McGuire, *Rev. Mod. Phys.* **25,** 279 (1953).
29. E. P. Trounson, D. F. Bleil, R. K. Wangsness, and L. R. Maxwell, *Phys. Rev.* **79,** 542 (1950).

30. L. Bonneviot and D. Olivier, *in* "Catalyst Characterisation—Physical Techniques for Solid Materials" (B. Imelik and J. C. Vedrine, Eds.), Chap. 7. Plenum Press, New York, 1994.
31. M. A. Alario-Franco, J. M. Thomas, and R. D. Shannon, *J. Solid State Chem.* **9,** 261 (1974).
32. W. H. Hartford, *Ind. Eng. Chem.* **41,** 1993 (1949).
33. B. Kubota, *J. Phys. Soc. Jpn.* **15,** 1706 (1960).
34. B. Kubota, *J. Am. Ceram. Soc.* **44,** 239 (1961).
35. R. S. Schwartz, I. Fankuchen, and R. J. Ward, *J. Am. Ceram. Soc.* **74,** 1676 (1952).
36. B. J. Thamer, R. M. Douglass, and E. Staritzky, *J. Am. Chem. Soc.* **79,** 547 (1957).
37. D. Rodbell and R. de Vries, *Mater. Res. Bull.* **2,** 491 (1967).
38. B. Kubota, *J. Am. Ceram. Soc.* **50,** 56 (1967).
39. R. Roy, *Bull. Soc. Chim. Fr.* 1065 (1965).
40. R. D. Shannon, *J. Am. Ceram. Soc.* **50,** 56 (1967).
41. F. J. Darnell and W. H. Cloud, *Bull. Soc. Chim. Fr.* 1164 (1965).
42. B. Kubota, A. Nishikava, A. Yause, E. Hivota, T. Michara, and Y. Iida, *J. Am. Ceram. Soc.* **46,** 550 (1963).
43. M. I. Zaki and N. E. Fouad, *Thermochim. Acta* **95,** 73 (1985).
44. J. D. Carruthers, K. S. W. Sing, and J. Fenerty, *Nature* **213,** 66 (1967).
45. T. A. Hewston and B. L. Chamberland, *J. Magn. Magn. Mat.* **43,** 89 (1984).
46. S. Okada, S. Kokubo, and K. Matsuo, *J. Soc. Chem. Ind. Jpn.* **46,** 324 (1943).
47. A. Ellison, G. Diakun, and P. Wothington, *J. Mol. Catal.* **131** (1988).